THE JOURNAL OF PHYSICAL CHEMISTRY A

Article

pubs.acs.org/JPCA

Hydrogen Recombination and Dimer Formation on Graphite from Ab Initio Molecular Dynamics Simulations

S. Casolo,[†] G. F. Tantardini,[†,‡] and R. Martinazzo*[,†,‡]

[†]Dipartimento di Chimica, Università degli Studi di Milano, via Golgi 19, 20133 Milan, Italy

[‡]Istituto di Scienze e Tecnologie Molecolari, CNR-ISTM, via Golgi 19, 20133 Milan, Italy

ABSTRACT: We studied Eley–Rideal molecular hydrogen formation on graphite using *ab initio* molecular dynamics, in the energy range relevant for the chemistry of the interstellar medium and for terrestrial experiments employing cold plasma (0.02–1 eV). We found substantial projectile steering effects that prevent dimer formation at low energies, thereby ruling out any catalytic synthetic pathways that form hydrogen molecules. *Ortho* and *para* dimers do form efficiently thanks to preferential sticking, but only at energies that are too high to be relevant for the chemistry of the interstellar medium. Computed reaction cross sections and ro-vibrational product populations are in good agreement with available experimental data and capable of generating adsorbate configurations similar to those observed with scanning tunneling microscopy techniques.

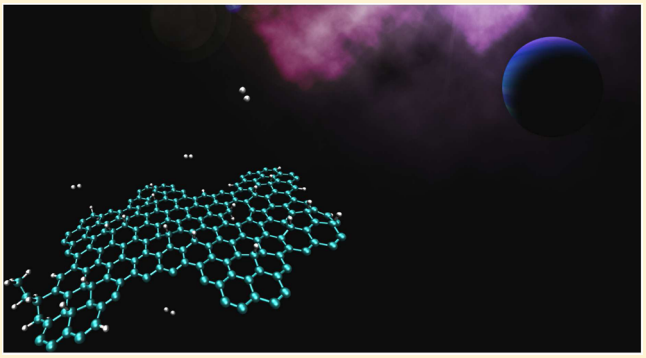

The interaction between hydrogen atoms and graphitic materials has been widely studied in the past decade, mainly because of its many applications in materials science and astrochemistry. After exposing semimetallic graphene to a cold hydrogen beam, it is possible to induce a band gap[1] forming either disordered[2−4] or locally crystalline hydrogenated phases such as graphane[5,6] or C_4H polymers.[7,8] At present H atom patterning is a very promising route to produce semiconducting graphene, and much effort has been devoted to study methods to design and control hydrogenation of this material.

In astrochemistry, molecular hydrogen is considered to be a key ingredient of the interstellar medium (ISM), because it is involved in both the formation of complex chemicals and the dynamics of the clouds. It was noticed that the star formation rate is related to the abundance of molecular gas, and in particular of H_2.[9,10] Hydrogen molecules are important cooling agents during the gravitational collapse of the clouds, despite the lack of a permanent dipole moment. H_2 is indeed by far the most abundant molecule present in the interstellar clouds that radiative cooling through weak quadrupole transitions is the main process allowing the collapse to continue until star ignition.

H_2 is found abundantly in both the *dense* and the *diffuse* molecular clouds of the ISM; therefore, an efficient route for H_2 production must be operative at the temperatures and densities typical of the ISM. Whereas gas-phase synthesis of H_2 is considered to be poorly efficient, a number of gas–surface pathways have been invoked that lead to a value of the recombination rate consistent with astronomical observations.[11]

The dust grains composition has been debated for long time, and many different models were proposed.[12] Among those models, structures based on silicate cores and sp^2 polycyclic aromatic hydrocarbons (PAH) should be good candidates and fit many observations, at least in warm environments, where icy mantles would quickly evaporate.[13,14] Therefore, many theoretical and experimental studies have focused on the H_2 recombination on graphitic surfaces for both physi- and chemisorbed H atoms. As physisorbed H atoms diffuse easily on the graphite surface, they may efficiently undergo Langmuir–Hinshelwood (LH) recombination, provided that the surface temperature (T_s) is lower than the desorption threshold (~40 K according to the physisorption well depth E_b ~ 40 meV, as obtained experimentally[15] and confirmed theoretically[16]). No chemisorption is expected in this regime, because H atoms need to overcome a barrier ~0.2 eV high to form a covalent bond, as a consequence of the rehybridization of the C atom valence orbitals from sp^2 to sp^3.[17,18] In warmer areas of the ISM, such as photon dominated (PDR) or shocked regions, the (gas) temperature ranges between 100 and 10 000 K, and only chemisorbed H atoms can be found. These species are immobile on the surface and do not suit to LH kinetics, thus foreshadowing a completely different scenario for hydrogen recombination. Sticking is difficult because of the above-mentioned adsorption barrier—though tunneling[19,20] and quantum fluctuations of the lattice[21] might help in this context—but is interesting because it is accompanied by some profound changes into the substrate. Indeed, formation of a CH

Special Issue: Piergiorgio Casavecchia and Antonio Lagana Festschrift

Received: December 31, 2015
Revised: February 23, 2016
Published: February 23, 2016

DOI: 10.1021/acs.jpca.5b12761
J. Phys. Chem. A 2016, 120, 5032−5040

bond leaves one unpaired electron on the lattice (a radical) that localizes mostly in the *ortho* and *para* positions, as a consequence of the aromaticiy of the substrate.[22] This is the reason for the preferential sticking mechanism forming *ortho* and *para* dimers on the carbon surface[23] (for a recent review see ref 24). Thus, in this case the possible recombination pathways are the Eley−Rideal (ER) abstraction between a chemisorbed H atom and a gas-phase H atom, a "hot-atom" recombination and the associative desorption of the H dimers.[25] Experimentally, the abstraction cross-section was found to have the same remarkably large value of about 4 Å^2 both in the high T_s and in the high coverage limit,[26,27] i.e., in conditions where hot-atom contributions are negligible. The thus estimated value of the ER cross section is much larger than that found for similar processes on semiconducting[28] and metallic[29] surfaces. This found a qualitative agreement with previous theoretical studies which, being mostly based on reduced models including only few degrees of freedom, were unable to account for the competing dimer formation process and for the energy transferred to the lattice.

In this work we studied the Eley−Rideal recombination of chemisorbed H atoms by means of *ab initio* molecular dynamics (AIMD), improving and extending our recent findings.[30] This approach allows us to quantify not only the cross section for the ER recombination but also that of the competing formation of many different dimer structures without the limitation of a static structureless substrate lattice. Differently from our previous investigation, we have extended the collision energy range investigated, the time scales considered, and we have tightened the simulation parameters. In addition, we analyzed the energy transfer to the surface and the effect of dispersion forces on the dynamics, and we included different isotopic combinations for the target and projectile H atoms.

We found that, at low energy, steering of the projectile atom gives an important contribution to the recombination, preventing dimer formation despite the favorable (barrierless) energetics. Only at higher energies are *para* and *ortho* dimers found to form abundantly, at the expense of the reaction yield. Computed cross sections and ro-vibrational H_2 populations are in good agreement with existing thermal desorption and molecular beams studies,[26] as well as with theoretical results obtained with different dynamical models.[31−33]

THEORETICAL METHODS

Ab initio (first-principles) molecular dynamics simulations were performed using the VASP package.[34,35] Exchange and correlation were treated at the generalized gradient approximation (GGA) level, with the PW91 functional[36] in its spin-polarized form. Core electrons were represented by ultrasoft pseudopotentials and the plane wave basis set was limited at 300 eV. The Brillouin zone was integrated on a 3 × 3 × 1 Γ-centered k points mesh and a 0.05 eV Gaussian smearing was used to ensure a fast electronic convergence. The graphite surface was modeled by a 3 × 3 single-layer graphene supercell consisting of 18 carbon atoms, and a vacuum layer 10 Å thick was introduced between periodic images to minimize their interaction. This setup was chosen to reproduce the energetics of a single H atom chemisorbed on graphite obtained in ref 22 but requires much less computational effort. Table 1 reports a comparison with literature data and shows that our setup allows a reasonable description of binding energies, chemisorption barriers and C−H bond lengths (in particular, the "puckering" height of the C atom out of the surface plane). In details, the

Table 1. Binding Energies (E_{bind}), Chemisorption Energy Barriers (E_{barr}), and Puckering Height (d_{puck}) for H Chemisorbed on Different Graphene Models

cell	E_{bind} (eV)	E_{barr} (eV)	d_{puck} (Å)	ref
2 × 2	0.67	0.20	0.36	18
coronene	0.57	0.16	0.35	17
3 × 3	0.77	0.20	0.42	22
3 × 3	0.84	0.20	0.50	this work
4 × 4	0.91			39
5 × 5	0.84	0.20	0.59	22

ER minimum energy path in this setup is barrierless, in agreement with recent studies,[37] whereas the formation of *para* dimers, also known to be barrierless,[38] is weakly activated (∼20 meV). However, because in the following we shall limit ourselves to collision energies higher than 20 meV, this spurious barrier is irrelevant for the reaction dynamics.

Dynamical simulations were performed by sampling the microcanonical (NVE) ensemble with classical trajectories. Hellmann−Feynman forces were computed on-the-fly with DFT whereas the Newton equations of motion were integrated using a Verlet algorithm, as implemented in VASP, with a time step dependent on the initial collision energy (E_{coll}): 0.40 fs for E_{coll} < 0.5 eV, 0.25 fs for 0.5 ≤ E_{coll} ≤ 0.8 eV, and 0.08 fs for E_{coll}> 0.8 eV.

At the beginning of each trajectory, the projectile atom was placed at 5 Å above the surface plane with (monochromatic) initial velocity directed along the surface normal. Only syn-facial adsorption was included in our simulation. The aiming points were generated by a uniform Monte Carlo sampling in a symmetry-irreducible sector $\theta = \pi/6$ of the circular area (r_{max} = 3.55 Å) centered around the target H atom. The surface initial conditions were not sampled in our calculations; instead each carbon atom and the target H were initially set at rest at their equilibrium positions and left free to move during the whole simulation. The only exceptions are the carbon atoms farthest away from the target, which were kept fixed along the axis normal to the surface plane to prevent block translations of the whole system after the impact with the projectile, thereby limiting the dynamical degrees of freedom (N) to N = 59. These initial conditions thus describe a surface initially at T_s = 0 K, which is appropriate for typical ISM conditions (e.g., T = 5−100 K in the interstellar clouds, and typically T_s < T); notice though that the Eley−Rideal reaction is expected to be little influenced by the surface temperature[32] and by the vibrational excitation of the target H atom.[40,41]

For each collision energy, we ran 500 trajectories, equivalent to 3000 trajectories on the whole circular area surrounding the target. The number of trajectories was increased to 1000 (per irreducible area) when rovibrational populations were computed at selected energies and isotopic substitutions. The reactive channels considered in the molecular dynamics simulations were the Eley−Rideal recombination (ER), dimer formation (DF), and collision-induced desorption. A dimer was considered as formed when the projectile H atom was found oscillating at a C site for at least seven vibrational periods. For the recombination channel, each product molecule was assigned to a rotational and vibrational state, based on standard binning into the rovibrational spectrum of the H_2 (HD) molecule, as obtained with the help of a discrete variable representation (DVR) Hamiltonian[42] on a Morse potential energy curve fit to data computed with the same DFT setup.

DOI: 10.1021/acs.jpca.5b12761
J. Phys. Chem. A 2016, 120, 5032−5040

It is worth mentioning at this point that collisions on the underlying adiabatic potential, which is dominated by the H−H interaction, result in a ER reaction only if the projectile and target atom spins are coupled as a singlet, triplet pairs experience a fully repulsive interaction.[43] Therefore, in our AIMD calculations we set the initial spins of the colliding pair (H-graphene and the gas-phase H atom) antiparallel, to help the system to follow the (ground state) singlet adiabatic surface, and scaled reactive AIMD cross sections by a spin statical factor 1/4. Similarly, for formation of *ortho* and *para* pairs, which occurs barrierless only in the (ground) singlet state.

RESULTS AND DISCUSSION

Eley−Rideal H_2 Recombination. Eley−Rideal recombination (abstraction) cross sections from AIMD simulations are shown in Figure 1 in the collision energy range 0.02−1.20 eV.

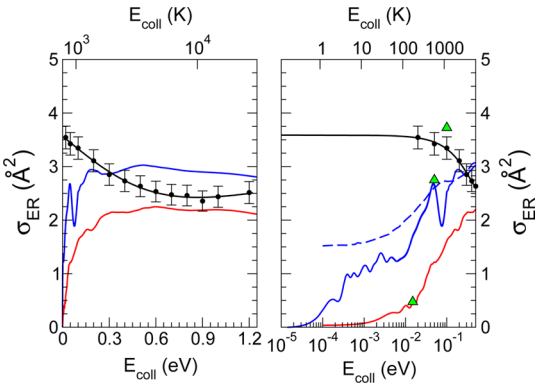

Figure 1. Left panel: cross sections for ER recombination from AIMD (black dots with error bars) and from quantum calculations within the adiabatic (blue) and sudden (red) rigid, flat-surface models.[31] Right panel: same graph shown in the low collision energy regime. Dashed line represents classical results obtained for the rigid, flat-surface adiabatic PES, and green triangles are for classical results on a Brenner-like potential.[44]

At low energy the abstraction cross sections are quite large (3.5 Å^2), and then decrease steadily to reach a plateau of 2.5 Å^2 at E_{coll} = 0.9 eV with a slight increase at higher energies. The ER-AIMD results can be compared with other classical and quantum studies performed on reduced-dimensionality models, to study the influence of the surface corrugation on the recombination dynamics. In the left panel of Figure 1 we show the quantum results obtained with a time dependent wave packet method on a three-dimensional model, corresponding to a *flat* and *rigid* graphite surface in two distinct dynamical regimes.[31] One is known as the "sudden" approximation and keeps the binding C atom frozen at its puckered position; this is expected to be appropriate at high collision energies, where the product molecule moves back to the gas phase on a time scale faster than the relaxation of the surface atom. The other is the so-called "adiabatic" approximation and takes the relaxed C atom height above the surface plane for each position of the two H atoms; this is expected to be more accurate at low collision energies where the carbon atom adjusts its position during the supposedly slow reaction dynamics.[18] Here we note that classical and quasi-classical results obtained from the same potentials give qualitatively the same results in regimes where quantum effects become negligible.[40]

It looks clear that at moderately high collision energies (E_{coll} > 0.6 eV) the AIMD results lie between the two curves obtained for the quantum reduced models, approaching the sudden results at E_{coll} ∼ 0.8−0.9 eV. At low energy, instead, a marked difference is observed. Two main factors contribute to this discrepancy. On the one hand, at vanishing collision energies the quantum cross sections vanish due to a quantum reflection effect, which occurs when the projectile de Broglie wavelength gets larger than the spatial variations of the attractive CH−H potential[31] (see, e.g., ref 45 for a surface science example). Classical calculations (either AIMD or QCT) are unable to account for this quantum effect and indeed show a reaction cross-section that levels off at some finite value when the projectile energy is reduced. On the other hand, AIMD calculations include the effects of surface corrugation and show an increasing cross-section at small collision energies. The flat, rigid-surface model underestimates reaction at low energies even in the classical limit (see the dashed line in the right panel of Figure 1). The same holds for the more accurate analytic representation of the interaction developed by Bachellerie et al.,[44] who used a Brenner-like potential model and included the lattice dynamics in their classical calculations. Both these models fail in describing the influence of the spin density excess localized on *ortho* and *para* positions with respect to the target atom, thereby suggesting that the *ortho*−*para* orientation effect plays a role not only in the formation of dimers but also in the ER recombination dynamics at low energies. This is made clear in Figure 2, which shows the location of the reactive aiming points at different values of E_{coll}. As is evident in that figure, at the lowest energy considered (E_{coll} = 20 meV, or 232 K), the aiming points of those trajectories leading to reaction are not isotropically distributed around the target atom but form a 3-fold shape protruded toward the *para* positions. This is a sign

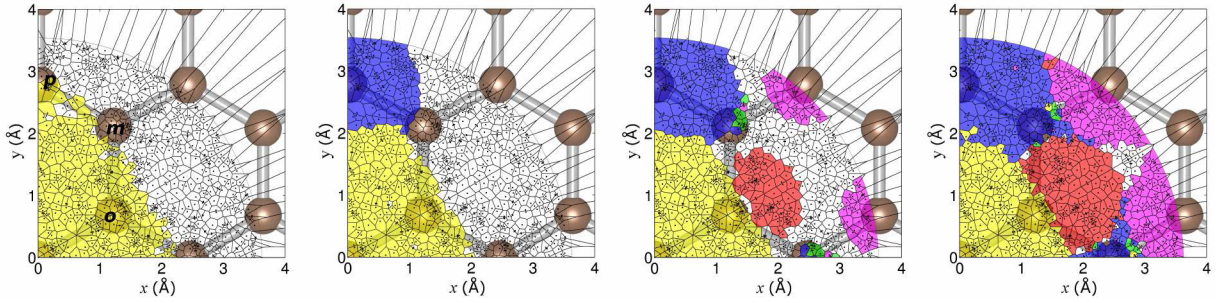

Figure 2. Aiming points location for AIMD trajectories at (from left to right) E_{coll} = 0.02, 0.2, 0.4, and 0.8 eV. The area around each aiming point was colored to match trajectories for ER (yellow), *ortho* dimer (red), *meta* dimer (green), *para* dimer (blue), and other dimers (magenta). The target H atom is located at the origin of the axes and the *ortho* (o), *meta* (m), and *para* (p) positions are indicated in the leftmost panel.

DOI: 10.1021/acs.jpca.5b12761
J. Phys. Chem. A 2016, 120, 5032−5040

that the attractive well generated by the unpaired electron is accelerating and *steering* the projectile atom toward the target atom, which then captures the projectile forming an H_2 molecule. This effect is less important at higher collision energies, where the projectile momentum becomes large compared to the attractive potential, and the ER reactive area gets progressively more isotropic.

Besides the direct abstraction of the target H atom we found other possible mechanisms for H_2 recombination. One is the abstraction by a projectile that is moving away from the surface after scattering off the repulsive potential of, e.g., a *meta* site, as shown in Figure 3. This "rebound" mechanism is different from

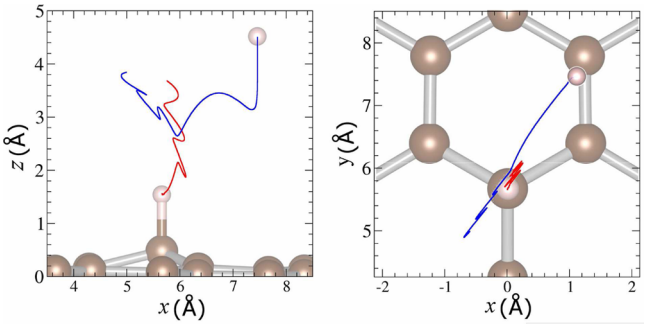

Figure 3. Typical "rebound" reactive trajectory in which the projectile H atom is first scattered by the repulsive potential of the meta C site, and then stirred toward the target H atom by its attractive potential.

that reported before for the flat and rigid model in which the abstraction takes place from below the target,[40] irrespective of the impact site. The other mechanism is the associative desorption from a metastable dimer pair in which the projectile atom sticks on the *para* site in a highly excited vibrational state and, after few vibrations, captures the target before dissipating its excess energy to the lattice. This mechanism was postulated in a recent study[46] and found in our AIMD trajectories only at $E_{coll} > 0.7$ eV. Unfortunately, the number of reactive trajectories is not large enough to provide the relative weight of each recombination mechanism with confidence; however, we estimate these last two pathways to be less than 10% of the total number of reactive trajectories.

At last, we note here that in the energy range considered here we found no exchange of the two H atom, nor any collision induced desorption, in agreement with previous studies.[40]

Dimer Formation. The most important DF cross sections are shown in Figure 4 as functions of E_{coll}, divided in *ortho*, *meta*, and *para*[a]. As already visible in Figure 2, at low energy the attractive potential of the target H atom hinders dimer formation in favor of reaction. Only increasing the collision energy some of the reactive trajectories turn into dimer formation, thereby determining a decrease of the ER recombination. DF cross sections rise slowly with energy until collisions get so fast that the projectile leaves the interaction region before the C atom has the time to move out from the surface plane and bind the projectile into a dimer.

The channels for the formation of H pairs open at different collision energies because of their different activation barrier, which in turn depends on the amount of spin density localized on the lattice site.[22] *Meta* dimers have a formation barrier comparable to that found when a hydrogen atom is adsorbed on a fresh surface, and their cross sections are much smaller than the *ortho* and *para* one, despite the larger number of sites

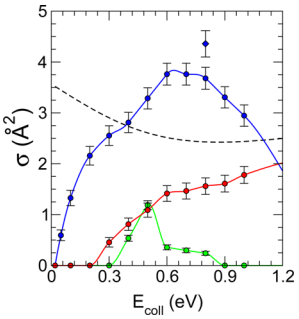

Figure 4. AIMD cross sections for the formation of H dimers: for the *ortho* (red), *meta* (green), and *para* (blue) dimers. The blue diamond shows the *para* dimer value obtained by doubling the sampled area (see text), and lines are guides to the eye. The dashed line is the ER cross section, set as a reference.

(six vs three) and the favorable spin statistics (triplet vs singlet). *Ortho* and *para* dimers have favorable energetics and present either a barrierless (*para*) or a weakly activated (*ortho*) path to their formation.[22] Dynamical results not only confirm that their formation is favored but also show that the dynamical threshold is larger than the adsorption barrier. The reason for this behavior, as mentioned above, is the competing reaction: the target atom lies about 2 Å above the surface plane and captures low energy projectiles (forming H_2) more efficiently than the *ortho* or *para* sites do.

Overall, *para* dimers are roughly twice as abundant as any other in the energy range considered, and at $E_{coll} < 0.2$ eV (2320 K) they are the only ones we found. From Figure 2 it is possible to notice that the sampled area is not large enough to enclose the whole *para*-forming region already at $E_{coll} = 0.2$ eV. The same holds of course for dimers lying further away from the nearest benzene ring; therefore, our σ_{DF} cross sections are best considered as lower bounds to the true values. To have a better estimate of the *para* cross section, we doubled the sampled area and the number trajectories at $E_{coll} = 0.8$ eV, where the DF reaches its maximum. We obtained an increase of 0.7 Å^2 in σ_{DF}, which is likely to be the error arising from truncating the sampled area to $r_{max} = 3.55$ Å.

Ortho dimers are the second most abundant species, and their cross section is the only one still increasing at $E_{coll} = 1.2$ eV. Curiously, their aiming points are not centered on-top to the *ortho* C atom;, instead they protrude toward the center of the adjacent benzene ring. This is a consequence of the shape of the interaction potential that forces the two atoms of the *ortho* dimer quite far from each other because of steric effects.[22,38,47]

Results from van der Waals-Corrected AIMD. When first-principles AIMD trajectories are computed, the results naturally reflect the lack of dispersive forces that standard DFT suffers. In the H-graphene system van der Waals (vdW) corrected functionals have been shown to improve the description of physisorption on graphene. In particular, it was recently shown that even the weak (~40 meV) physisorption well of H atoms on PAHs could be reasonably reproduced by including simple corrections to the DFT functionals.[38,48] Therefore, we further ran AIMD trajectories using the PW91 functional with the additional Grimme's DFT-D2 van der Waals parametric corrections[49] in the range 0.02 eV < E_{coll} < 0.5 eV. The results of these calculations are shown in Figure 5.

For the case of the ER reactive channel, the van der Waals corrected results are significantly different from the non-

DOI: 10.1021/acs.jpca.5b12761
J. Phys. Chem. A 2016, 120, 5032−5040

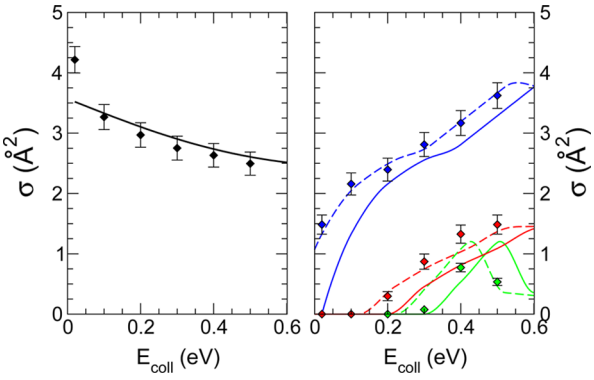

Figure 5. Effect of the van der Waals corrections to cross sections at low energies on ER (left panel) and DF (right) cross sections. Results for ER and for *ortho*, *meta*, and *para* DF are given in black, red, green, and blue, respectively. Diamonds show the vdW-corrected AIMD results, full lines show the AIMD results of Figure 1 and 4, and dashed lines show the same results shifted by −80 meV.

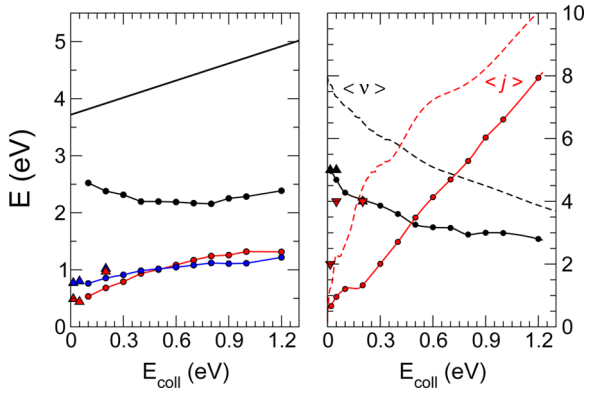

Figure 6. Left panel: partitioning of the reaction energy into surface degrees of freedom (blue), H_2 center of mass (red), and H_2 internal (black) motion. The black line shows the total energy of the system (ΔH_{react} + E_{coll}). Right panel: average H_2 vibrational (black) and rotational (red) quantum number as obtained from AIMD (dots-full lines) and quantum (dashed lines) calculations. Triangles are classical trajectory results from ref 44; color codes follow those of AIMD data.

corrected ones only at E_{coll} = 0.02 eV, for which σ_{ER} is increased by 0.67 Å^2. This is consistent with recent kinetic Monte Carlo simulations, which estimated the effect of steering in the abstraction process in about 1 Å^2 of the cross-section[50] (once corrected for the spin statistics). The enhanced reactivity comes from an enlargement of the capture radius of the target H atom, which follows from the increased interaction of the projectile with the surface.

In contrast, the DF cross sections increase in the whole energy range considered, and their thresholds move toward lower energy, eventually disappearing (see the case of the *para* dimers in Figure 5). This effect is due to the lowering of the chemisorption barriers and the increased attractive potential due to the DFT-D2 contribution. At a closer inspection it is possible to notice that the van der Waals corrected results can be reproduced by shifting toward low energies the uncorrected ones by 80 meV. Therefore, we can infer that the correction has the effect of accelerating the projectile by this amount.

It should be noted though that the effect of the vdW forces is likely to be overemphasized with the adopted correction. Although necessary for reproducing the physisorption well far from the surface the effect of Grimme's D2 correction extends indeed to much smaller values of the height of the projectile above the surface. The vdW correction reduces the adsorption barrier and increases the chemisorption energy,[20] at odds with the long-range nature of the vdW interactions. Particularly important is the effect on the barrier to sticking, because the latter already suffers from a general underestimation due to the use of a semilocal functional[51] and is likely to be better reproduced without such correction. Better results are expected from the use of vdW-functionals, which though are not yet practical for AIMD if a good statistics is required.

Energy Budget. The reaction enthalpy for the recombination process is

$$C(gr)H \rightarrow H(g) + C(gr) \qquad \Delta E = 0.84 \text{ eV} \tag{1}$$

$$H(g) + H(g) \rightarrow H_2(g) \qquad \Delta E = -4.50 \text{ eV} \tag{2}$$

$$\Delta E_{react} = 0.84 \text{ eV} - 4.50 \text{ eV} = -3.76 \text{ eV} \tag{3}$$

The partitioning of the reaction energy *plus* the collision energy into surface and molecular degrees of freedom is shown in Figure 6. Most of the reaction energy is stored in the product internal (vibrational and rotational) degrees of freedom; i.e., product molecules are rovibrationally hot, consistently with many previous findings.[31−33,40]

The energy transfer to the surface is about 20% of the available energy, in agreement with the findings of ref 44. It changes only slowly with increasing E_{coll} and is generally larger than that found in other studies, which limited somewhat the surface atoms motion.[52,53] Interestingly, the amount of energy left on the surface (∼0.9−1.0 eV) compares rather well with the puckering energy, i.e., the energy needed to move the C atom out of the pristine surface at a height it has when it binds a hydrogen atom. This shows that reaction is close to the sudden limit: the molecular product is formed on a time scale shorter than the one needed for surface relaxation, the carbon atom remains essentially frozen in its puckered configuration, and only at later times, when H_2 is far away from the surface, does it release its excess energy. The slight increase with collision energy is caused by the additional energy transfer due to the impulsive collision of the projectile.

Importantly, the energy transferred to the lattice is significant, and the formation of hydrogen molecules considerably heats the interstellar grains. Using the low temperature Debye expression of the specific heat, $c_v = 12\pi^4/5 \times n \times k_B \times (T/\Theta_D)^3$, where $n \sim 4/35.3 \times 10^{30}$ m^{-3} is the number density of carbon atoms in graphite and $\Theta_D \sim 400$ K is its Debye temperature,[54] we estimate that formation of a *single* H_2 molecule on a grain 1 μm^3 sized at T = 5 K increases its temperature by 2.2×10^{-4} K.

The internal energy of the product molecule initially decreases and then increases from around 0.6 eV. This behavior may be understood by looking at the average vibrational and rotational quantum numbers of the nascent H_2. At low collision energies the product is mostly vibrationally hot and rotationally cold. At higher energies rotational excitation increases quickly as the vibrational one decreases, as more large-impact-parameter trajectories rebounding on the repulsive potential of the surface gets captured by the target (see Figure 3 and the section "Eley−Rideal H_2 Recombination"). The values for $\langle v \rangle$ and $\langle j \rangle$ are significantly smaller than those obtained with quantum calculations in the rigid surface approximation,[31] though present a similar dependence on the collision energy.

DOI: 10.1021/acs.jpca.5b12761
J. Phys. Chem. A 2016, 120, 5032−5040

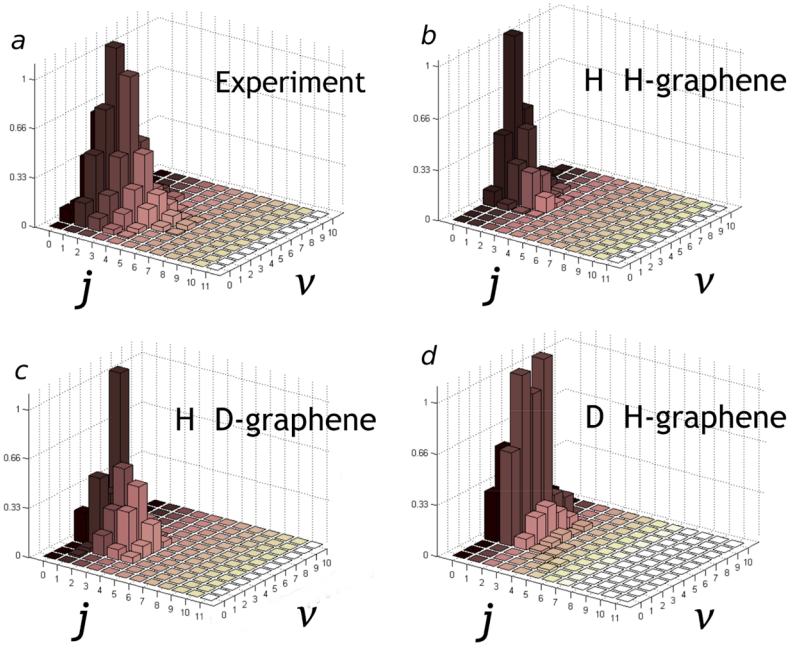

Figure 7. Relative ro-vibrational population for the product molecule: (a) Experimental results from ref 55 for the recombination of H and D beams (T_{gas} = 300 K) on HOPG kept at T_{surf} = 15 K;p (b−d) AIMD results at E_{coll} = 20 meV (∼230 K) for H impinging on chemisorbed H, H on D, and D on H, respectively.

This effect could be anticipated, because the graphite surface dissipates part of the reaction energy by exciting phonons. Nevertheless, our AIMD results for the average rotational quantum number of H_2 are also smaller than those obtained using the Brenner-like potential,[44] thereby suggesting that the attractive well localized on the para site affects not only the cross section but also the detailed dynamics of molecular formation.

Comparison with Experiments. The AIMD cross sections can be compared with those obtained experimentally by integrating the peaks of thermal desorption spectroscopy (TDS) profiles. In these experiments, an atomic beam of hydrogen atoms is directed toward a HOPG (highly oriented pyrrolytic graphite) surface that has been previously exposed to D atoms, at different coverages. In these conditions, other reaction mechanisms cannot be excluded *a priori*, in particular hot-atom (HA) recombination was found to be efficient for H on metals and should be expected for graphite as well.[56] Indeed, TDS data for HOPG[26] are similar to those for the Cu(111) surface, in which HD formation rate does rise linearly with the coverage (as expected for an ER process) but because of formation of HAs with a preference for reaction over sticking. Graphite has a physisorption well of about 40 meV,[15,16] which may host fast diffusing projectiles. In this scenario, a HA mechanism cannot be excluded and may also explain the detection of D_2 molecules.[26] To remove the HA fraction from the experimental cross sections, we take as a reference the (same) limiting value observed either at high surface temperatures or at a high D coverage.[27] In these conditions HAs cannot contribute to the reaction either because they desorb before encountering their reaction partner or because the crowd of H atom makes ER much more likely. At saturation D precoverage (Θ = 0.4 ML) the recombination cross-section gets independent of the surface temperature[26] and levels off at the same value obtained at a high T_s value (400 K),[27] about 3.75 Å^2 for a hyperthermal beam at $T \sim$ 2000 K. We compare this value with that obtained with AIMD at a collision energy of 0.2 eV, the closest to the corresponding maximum of the Maxwell−Boltzmann distribution of the experimental H sources. At the surface coverage of the simulation (θ = 1/18 ML ≃ 0.055 ML) after running 1000 trajectories per irreducible area we obtain σ_{ER} = 3.77 ± 0.15 Å^2 for H impinging on H, σ_{ER} = 3.92 ± 0.15 Å^2 for H impinging on D, and σ_{ER} = 3.99 ± 0.15 Å^2 for D impinging on H. The agreement is rather good, despite the simulated conditions are not exactly the same as the experimental ones.

Some more experimental data are available for the population of ro-vibrational states of the nascent molecular product.[55,57,58] In this series of studies, H atoms with a mean energy of 300 K recombine with pre-dosed D atoms on a graphite surface at 15 K and product HD internal state are probed with laser spectroscopy. A comparison of experimental and AIMD results at E_{coll} = 20 meV is shown in Figure 7. Experiments found most of the products in a low-lying rotational state, while they have a significant vibrational excitation. Our simulations reproduce semiquantitatively this behavior and show rather peaked distributions with dominant contributions from the state ν = 5, j = 1 for H on D and from ν = 5, j = 0 for H on H. For D impinging on chemisorbed H, however, we found a much broader distribution, though still peaked at a low rotational and at high vibrational quantum numbers ((j, ν) = (1, 4−6)). Overall, our results are in rather good agreement with the experiments, with only minor deviations from the experimentally determined rovibrational distributions.[55,57,58] This suggests that, under the above-described experimental conditions, ER recombination dominates over LH: if the reaction followed Langmuir−Hinshelwood kinetics, H_2 product molecules would be rotationally hot.[59,60] Hence, the low surface temperature used in the experiment prevents physisorbed species to desorb but cannot preclude trapping in (facile) chemisorption sites where direct ER recombination with a gas phase atom can occur.

DOI: 10.1021/acs.jpca.5b12761
J. Phys. Chem. A 2016, 120, 5032−5040

Quantitative data for dimer formation are still lacking, although some information may be inferred from STM experiments and vibrational spectroscopy. From our AIMD results we expect that Eley−Rideal recombination dominates at low energy, where the *para* DF cross section is found to be much smaller than the ER one. This is in qualitative agreement with recent experiments in which a HOPG surface precovered with D atoms is observed to form dimers and clusters only when irradiated with highly energetic H atoms,[61] whereas at low energy (E_{coll} = 25 meV) only ER abstraction occurs.[62] These data also suggest that the use of van der Waals interaction in the AIMD does not improve the quality of the simulations, because it promotes dimer formation even at very low collision energies. Unfortunately, in our simulations formation of *ortho* dimers was found to be efficient only at $E_{coll} \geq 0.3$ eV, whereas in experiments such dimers were found to be already abundant at this energy. Hence, in this case the vdW corrections would improve the AIMD simulations, thereby contradicting the previous case. This finding signals the need of a higher correlation level in the simulations which can overcome the limits of the semilocal functionals and of an empirical vdW correction.

The AIMD results have also an important application for the chemistry of the ISM, where H_2 probably forms via recombination of chemisorbed species. Because *para* DF is a barrierless process, in principle, it may initiate a catalytic cycle on the graphitic dust grains. In this process a chemisorbed H atom first pairs with a H atom to form a *para* dimer via barrierless adsorption, then it undergoes ER abstraction (also barrierless) to produce H_2 and returns to the original configuration.[23] This efficient synthetic pathway would explain the high abundance of H_2 molecules in diffuse clouds, but our results clearly show that at the gas temperatures relevant for the ISM clouds (10−100 K, i.e., 10^{-4}−0.01 eV) no dimer formation occurs. Therefore, this suggestive hypothesis is only plausible at the higher temperatures of PDR or shocked regions where DF can effectively compete with ER abstraction.

SUMMARY AND CONCLUSIONS

We studied the dynamics of H atoms on a graphene surface including the full lattice corrugation and its motion with the help of *ab initio* molecular dynamics. We computed cross sections for Eley−Rideal recombination and for the competing dimer formation channel, showing that at low collision energies the H_2 formation is a very efficient process due to projectile steering. At energies larger than 0.3 eV the formation of H dimers dominates, and *para* dimers are found to form twice as much as any other dimer species. We critically analyzed the role of vdW corrections and determined the energy transferred to the lattice. Our findings suggest that molecular formation via ER recombination considerably heats the interstellar grains, releasing the puckering energy initially stored in the surface when chemisorbing the target atom. We further computed detailed ro-vibrational distributions at selected energies for different isotopic combinations and compared our results with existing experiments. Reaction cross sections and product H_2 ro-vibrational populations were found to be in good agreement with experimental results, proving that AIMD is a reliable method to study complex reactions at surfaces, where most often many competing channels need to be taken into account.

AUTHOR INFORMATION

Corresponding Author

*R. Martinazzo. E-mail: rocco.martinazzo@unimi.it. Phone: +39 0250314287.

Notes

The authors declare no competing financial interest.

ACKNOWLEDGMENTS

This work has been supported by Regione Lombardia and CINECA through a Laboratory for Interdisciplinary Advanced Simulation (LISA) Initiative grant (2014).

ADDITIONAL NOTE

[a]Because the ground-state *meta* dimers are in a *triplet* state and our AIMD trajectories follow the lowest energy adiabatic surface, we used a different spin statistical factor (3/4) for this dimer configuration

REFERENCES

(1) Bostwick, A.; McChesney, J.; Seyller, K. E. T.; Horn, K.; Kevan, S. D.; Rotenberg, E. Quasiparticle Transformation During a Metal-Insulator Transition In Graphene. *Phys. Rev. Lett.* **2009**, *103*, 56404−56408.

(2) Bangert, U.; Pan, C. T.; Nair, R. R.; Gass, M. H. Structure of Hydrogen-dosed Graphene Deduced from Low Electron Energy Loss Characteristics and Density Functional Calculations. *Appl. Phys. Lett.* **2010**, *97*, 253118−253122.

(3) Eren, B.; Hug, D.; Marot, L.; Pawlak, R.; Kisiel, M.; Steiner, R.; Zumbül, D. M.; Meyer, E. Pure Hydrogen Low-Temperature Plasma Exposure of HOPG and Graphene: Graphane Formation? *Beilstein J. Nanotechnol.* **2012**, *3*, 852−859.

(4) Burgess, J. S.; Matis, B. R.; Robinson, J. T.; Bulat, F. A.; Perkins, F. K.; Houston, B. H.; Baldwin, J. W. Tuning The Electronic Properties of Graphene by Hydrogenation in a Plasma Enhanced Chemical Vapor Deposition Reactor. *Carbon* **2011**, *49*, 4420−4426.

(5) Sofo, J. O.; Chaudhari, A. S.; Barber, G. D. Graphane: a Two-Dimensional Hydrocarbon. *Phys. Rev. B: Condens. Matter Mater. Phys.* **2007**, *75*, 153401−153405.

(6) Elias, D. C.; Nair, R. R.; Mohiuddin, T. M. G.; Morozov, S. V.; Blake, P.; Halsall, M. P.; Ferrari, A. C.; Boukhvalov, D. W.; Katsnelson, M. I.; Geim, A. K.; et al. Control of Graphene's Properties by Reversible Hydrogenation: Evidence for Graphane. *Science* **2009**, *323*, 610−613.

(7) Haberer, D.; Giusca, C. E.; Wang, Y.; Sachdev, H.; Farjam, A. V. F. M.; Vyalikh, S. A. J. D. V.; Usachov, D.; Liu, X.; Treske, U.; Grobosch, M.; et al. Evidence of a New Two-Dimensional C4H Type Polymer Based on Graphene. *Adv. Mater.* **2011**, *23*, 4497−4503.

(8) Siemer, B.; Olsen, T.; Hoger, T.; Rutowski, M.; Thewes, C.; Düsterer, S.; Schiøtz, J.; Zacharias, H. Desorption of H Atoms From Graphite (0001) Using XUV Free Electron Laser Pulses. *Chem. Phys. Lett.* **2010**, *500*, 291−294.

(9) Leroy, A. K.; Walter, F.; Brinks, E.; Bigiel, F.; de Blok, W. J. G.; Madore, B. F.; Thornley, M. D. The Star Formation Efficiency in Nearby Galaxies: Measuring Where Gas Forms Stars Effectively. *Astron. J.* **2008**, *136*, 2782−2845.

(10) Kennicutt, R. C.; Evans, N. J. Star Formation In The Milky Way and Nearby Galaxies. *Annu. Rev. Astron. Astrophys.* **2012**, *50*, 531−608.

(11) Hollenbach, D. J.; Salpeter, E. E. Surface Recombination of Hydrogen Molecules. *Astrophys. J.* **1971**, *163*, 155−164.

(12) Voshchinnikov, N. V. Interstellar Exctincion and Polarization: Old and New Models. *J. Quant. Spectrosc. Radiat. Transfer* **2012**, *113*, 2334−2350.

(13) Papoular, R.; Conrad, J.; Guillois, O.; Nenner, I.; Reynaud, C.; Rouzaud, J. N. A Comparison of Solid-State Carbonaceous Models of Cosmic Dust. *Astron. Astrophys.* **1996**, *315*, 222−236.

DOI: 10.1021/acs.jpca.5b12761
J. Phys. Chem. A 2016, 120, 5032−5040

(14) Li, A.; Greenberg, J. M. A Unified Model of Interstellar Dust. *Astron. Astrophys.* **1997**, *323*, 566−584.
(15) Ghio, E.; Mattera, L.; Salvo, C.; Tommasini, F.; Valbusa, U. Vibrational Spectrum of H and D on The (0001) Graphite Surface From Scattering Experiment. *J. Chem. Phys.* **1980**, *73*, 556−565.
(16) Bonfanti, M.; Martinazzo, R.; Tantardini, G. F.; Ponti, A. Physisorption and Diffusion of Hydrogen Atoms on Graphite From Correlated Calculations on The H-Coronene Model System. *J. Phys. Chem. C* **2007**, *111*, 5825−5829.
(17) Jeloaica, L.; Sidis, V. DFT Investigation of The Adsorption of Atomic Hydrogen on a Cluster-Model Graphite Surface. *Chem. Phys. Lett.* **1999**, *300*, 157−162.
(18) Sha, X.; Jackson, B. First-Principles Study of The Structural and Energetic Properties of H Atoms on a Graphite (0001) Surface. *Surf. Sci.* **2002**, *496*, 318−330.
(19) Goumans, T. P. M.; Kästner, J. Hydrogen-Atom Tunneling Could Contibute To H_2 Formation. *Angew. Chem., Int. Ed.* **2010**, *49*, 7350−7352.
(20) Davidson, E. R. M.; Klime, J.; Alfè, D.; Michaelides, A. Cooperative Interplay of van Der Waals Forces and Quantum Nuclear Effects on Adsorption: H At Graphene and At Coronene. *ACS Nano* **2014**, *8*, 9905−9913.
(21) Bonfanti, M.; Jackson, B.; Hughes, K. H.; Burghardt, I.; Martinazzo, R. Quantum Dynamics of Hydrogen Atoms on Graphene. II. Sticking. *J. Chem. Phys.* **2015**, *143*, 124704−124704.
(22) Casolo, S.; Løvvik, O. M.; Martinazzo, R.; Tantardini, G. F. Understanding Adsorption of Hydrogen Atoms on Graphene. *J. Chem. Phys.* **2009**, *130*, 054704−054704.
(23) Hornekær, L.; Rauls, E.; Xu, W.; Šljivančanin, Ž; Otero, R.; Stensgaard, I.; Lægsgaard, E.; Hammer, B.; Besenbacher, F. Clustering of Chemisorbed H(D) Atoms on The Graphite (0001) Surface Due To Preferential Sticking. *Phys. Rev. Lett.* **2006**, *97*, 186102−186105.
(24) Martinazzo, R.; Casolo, S.; Hornekær, L. In *Dynamics of Gas-Surface Interactions*; Diez-Muiño, R., Busnengo, F. H., Eds.; Springer: Berlin, 2013; pp 157−178.
(25) Hornekær, L.; Šljivančanin, Ž.; Xu, W.; Otero, R.; Rauls, E.; Stensgaard, I.; Lægsgaard, E.; Hammer, B.; Besenbacher, F. Metastable Structure and Recombination Pathways for Atomic Hydrogen on The Graphite (0001) Surface. *Phys. Rev. Lett.* **2006**, *96*, 156104−156108.
(26) Zecho, T.; Güttler, A.; Sha, X.; Lemoine, D.; Jackson, B.; Küppers, J. Abstraction of D Chemisorbed on Graphite (0001) with Gaseous H Atoms. *Chem. Phys. Lett.* **2002**, *366*, 188−195.
(27) Zecho, T. Personal communication, 2008.
(28) Dinger, A.; Lutterloh, C.; Küppers, J. Kinetics of D Abstraction with H Atoms From The Monodeuteride Phase on Si(100) Surfaces. *Chem. Phys. Lett.* **1999**, *311*, 202−208.
(29) Martinazzo, R.; Assoni, S.; Marinoni, G.; Tantardini, G. Hot-Atom Versus Eley-Rideal Dynamics In Hydrogen Recombination on Ni(100). The single Adsorbate Case. *J. Chem. Phys.* **2004**, *120*, 8761−8772.
(30) Casolo, S.; Tantardini, G.; Martinazzo, R. Insights Into H_2 Formation In Space From Ab Initio Molecular Dynamics. *Proc. Natl. Acad. Sci. U. S. A.* **2013**, *110*, 6674−6677.
(31) Casolo, S.; Martinazzo, R.; Bonfanti, M.; Tantardini, G. F. Quantum Dynamics Of The Eley-Rideal Hydrogen Formation Reaction on Graphite At Typical Interstellar Cloud Conditions. *J. Phys. Chem. A* **2009**, *113*, 14545−14553.
(32) Sizun, M.; Bachellerie, D.; Anguillon, F.; Sidis, V. Investigation of ZPE and Temperature Effects on The Eley-Rideal Recombination of Hydrogen Atom In Graphene Using a Multidimensional Graphene H-H Potential. *Chem. Phys. Lett.* **2010**, *498*, 32−37.
(33) Sha, X.; Jackson, B.; Lemoine, D.; Lepetit, B. Quantum studies of H atom trapping on a graphite surface. *J. Chem. Phys.* **2005**, *122*, 014709−014715.
(34) Kresse, G.; Hafner, J. Ab Initio Molecular-Dynamics Simulation of The Liquid-Metal-Amorphous-Semiconductor Transition In Germanium. *Phys. Rev. B: Condens. Matter Mater. Phys.* **1994**, *49*, 14251−14258.
(35) Kresse, G.; Hafner, J. Ab Initio Molecular Dynamics for Liquid Metals. *Phys. Rev. B: Condens. Matter Mater. Phys.* **1993**, *47*, 558−561.
(36) Perdew, J.; Chevary, J.; Vosko, S.; Jackson, K.; Pederson, M.; Singh, D.; Fiolhais, C. Atoms, Molecules, Solids, and Surfaces: Applications of The Generalized Gradient Approximation for Exchange and Correlation. *Phys. Rev. B: Condens. Matter Mater. Phys.* **1992**, *46*, 6671−6680.
(37) Bonfanti, M.; Casolo, S.; Tantardini, G. F.; Martinazzo, R. Surface Models and Reaction Barrier in Eley-Rideal formation of H_2 on Graphitic Surfaces. *Phys. Chem. Chem. Phys.* **2011**, *13*, 16680−16688.
(38) Rougeau, N.; Teillet-Billy, D.; Sidis, V. on The PES for The Interaction Of An H Atom with An H Chemisorbate on a Graphenic Platelet. *Phys. Chem. Chem. Phys.* **2011**, *13*, 17579−17587.
(39) Hsing, C.; Wei, C.; Chou, M. Quantum Monte Carlo Investigations of Adsorption Energetics on Graphene. *J. Phys.: Condens. Matter* **2012**, *24*, 395002−395009.
(40) Martinazzo, R.; Tantardini, G. F. Quantum study of Eley-Rideal Reaction and CID of Hydrogen on a Graphite Surface. I Chemisorbed Case. *J. Chem. Phys.* **2006**, *124*, 124702.
(41) Martinazzo, R.; Tantardini, G. F. Quantum Study of Eley-Rideal Reaction and CID of Hydrogen on a Graphite Surface. II Physisorbed Case. *J. Chem. Phys.* **2006**, *124*, 124703−124703.
(42) Colbert, D. T.; Miller, W. H. A Novel DVR for Quantum Mechanical Reactive Scattering Via S-Matrix Kohn Method. *J. Chem. Phys.* **1992**, *96*, 1982−1991.
(43) Sharp, T. E. Potential Energy Curves for Molecular Hydrogen and Its Ions. *At. Data Nucl. Data Tables* **1970**, *2*, 119−169.
(44) Bachellerie, D.; Sizun, M.; Anguillon, F.; Teillet-Billy, D.; Rougeau, N.; Sidis, V. Unrestricted study of the Eley−Rideal formation of H_2 on graphene using a new multidimensional graphene−H−H potential: role of the substrate. *Phys. Chem. Chem. Phys.* **2009**, *11*, 2715−2729.
(45) Oberst, H.; Tashiro, Y.; Shimizu, K.; Shimizu, F. Quantum Reflection of He* On Silicon. *Phys. Rev. A: At., Mol., Opt. Phys.* **2005**, *71*, 052901−052907.
(46) Cuppen, H. M.; Hornekær, L. Kinetic Monte Carlo Studies of Hydrogen Abstraction Reaction From Graphite. *J. Chem. Phys.* **2008**, *128*, 174707−174707.
(47) Rogeau, N.; Teillet-Billy, D.; Sidis, V. Double H Atom Adsorpition on A cluster Model of a Graphite Surface. *Chem. Phys. Lett.* **2006**, *431*, 135−138.
(48) Ferullo, R. M.; Domancich, N. F.; Castellani, N. J. On The Performance of Van Der Waals Corrected Density Functional Theory In Describing Atomic Hydrogen Physisorption on Graphite. *Chem. Phys. Lett.* **2010**, *500*, 283−286.
(49) Grimme, S. Semiempirical GGA-type Density Functional Constructed with a Long Range Dispersion Correction. *J. Comput. Chem.* **2006**, *27*, 1787−1799.
(50) Gavardi, E.; Cuppen, H. M.; Hornekær, L. A Kinetic Monte Carlo Study Of Desorption of H_2 From Graphite (0001). *Chem. Phys. Lett.* **2009**, *477*, 285−289.
(51) Wang, Y.; Qian, H.-J.; Morokuma, K.; Irle, S. Coupled Cluster and Density Functional Theory Calculations of Atomic Hydrogen Chemisorption on Pyrene and Coronene as Model Systems for Graphene Hydrogenation. *J. Phys. Chem. A* **2012**, *116*, 7154−7160.
(52) Ree, J.; Kim, Y.; Shin, H. Reactions of Gas-Phase Atomic Hydrogen with Chemisorbed Hydrogen on a Graphite Surface. *Bull. Korean Chem. Soc.* **2007**, *28*, 635−646.
(53) Rutigliano, M.; Cacciatore, M. Isotope and Surface Temperature Effects for Hydrogen Recombination on a Graphite Surface. *ChemPhysChem* **2008**, *9*, 171−181.
(54) Tohei, T.; Kuwabara, A.; Oba, F.; Tanaka, I. Debye Temperature and Stiffness of Carbon and Boron Nitride Polymorphs from First Principles Calculations. *Phys. Rev. B: Condens. Matter Mater. Phys.* **2006**, *73*, 064304−064310.
(55) Latimer, E. R.; Islam, F.; Price, S. D. Studies of HD Formed in Excited Vibrational States from Atomic Recombination on Cold Graphite Surfaces. *Chem. Phys. Lett.* **2008**, *455*, 174−177.

DOI: 10.1021/acs.jpca.5b12761
J. Phys. Chem. A 2016, 120, 5032−5040

(56) Kammler, T.; Kolovos-Vellianitis, D.; Küppers, J. A Hot-Atom Reaction Model for H Abstraction from Solid Surfaces. *Surf. Sci.* **2000**, *460*, 91−100.
(57) Creighan, S. C.; Perry, J. S.; Price, S. D. The Rovibrational Distribution of H_2 and HD Formed on a Graphite Surface at 15 K. *J. Chem. Phys.* **2006**, *124*, 114701−114701.
(58) Islam, F.; Latimer, E. R.; Price, S. D. The Formation of Vibrationally Excited HD from Atomic Recombination on Cold Graphite Surfaces. *J. Chem. Phys.* **2007**, *127*, 064701−064701.
(59) Morisset, S.; Aguillon, F.; Sizun, M.; Sidis, V. Quantum dynamics of H_2 Formation on a Graphite Surface Through the Langmuir Hinshelwood Mechanism. *J. Chem. Phys.* **2004**, *121*, 6493−6501.
(60) Morisset, S.; Aguillon, F.; Sizun, M.; Sidis, V. Wave-packet Study of H_2 Formation on a Graphite Surface Through the Langmuir-Hinshelwood mechanism. *J. Chem. Phys.* **2005**, *122*, 194702−194702.
(61) Thomas, C.; Angot, T.; Layet, J. Investigation of D(H) Abstraction by Means of HR-EELS. *Surf. Sci.* **2008**, *602*, 2311−2314.
(62) Areou, E.; Carty, G.; Layet, J.; Angot, T. Hydrogen-Graphite Interaction: Experimental Evidences of an Adsorption Barrier. *J. Chem. Phys.* **2011**, *134*, 014701−014701.

DOI: 10.1021/acs.jpca.5b12761
J. Phys. Chem. A 2016, 120, 5032−5040